PHYSICAL REVIEW A VOLUME 16, NUMBER 1 JULY 1977

Light drag in a ring laser: An improved determination of the drag coefficient

H. R. Bilger* and W. K. Stowell†

School of Electrical Engineering, Oklahoma State University, Stillwater, Oklahoma 74074

(Received 20 July 1976)

The light drag in a rotating fused-silica disk inserted in a He-Ne ring laser was measured at $\lambda = 633$ nm and found to be $\alpha_e = 0.5424$ with an rms error (1σ) of $\pm 2\times 10^{-4}$, including the known error sources. This constitutes a tenfold improvement in accuracy over a previous result. While the given error margin does not include the value given by the Lorentz drag in a linear arrangement, $\alpha_{LO} = 0.541\,82$, the measured difference of 2σ is deemed too small to claim a discrepancy.

I. INTRODUCTION

Determinations of light drag require a differential sensor, as the classical experiments of Fizeau, Michelson and Morley, and Zeeman demonstrate.[1] The ring laser satisfies such a requirement par excellence, by virtue of the contracirculating beams. Macek *et al.*[2] were the first to demonstrate the drag effect in ring lasers. Recently, a measurement of the drag coefficient in a rotating fused silica disk was accomplished[3] with an accuracy of $\pm 0.6\%$. This constituted over an order of magnitude of improvement in accuracy over Zeeman's experiments with quartz,[4] and showed at once the potential of the ring laser for precision drag experiments. The error was sufficiently small to show that the drag coefficient was substantially different from the value as calculated by the original Fresnel formula. It was considered desirable, however, to improve on the accuracy in order to determine (i) which of the various formulations of the dispersion terms correctly describe results obtained with a specific geometry of the drag medium, and (ii) more fundamentally, whether the simple transplant from classical linear arrangements to a ring laser (closed light path, self-oscillating, noninertial situation) is valid.

Details of the drag theory are given in Sec. II. Careful attention is given to error sources since an overall error of less than $\pm 0.1\%$ is to be achieved. This all-important aspect of this paper is discussed in Sec. III. Experimental results are given in Sec. IV. The remainder contains an analysis of the drag effect, a quantitative estimate of errors, a comparison with theory, and a discussion of the significance of the results.

II. DRAG IN A RING LASER

The experimental situation is summarized in Fig. 1: A triangular ring laser has in its light path (I) a cylindrical fused silica disk which is tilted relative to the incident ring-laser beam by an angle $\xi = \theta$; ideally, $\xi = \theta_B$ (Brewster angle). The orientation angle ϕ (ideally, $\phi = 90°$) is the angle between the plane defined by the face of the disk and the plane perpendicular to the plane of the ring laser and coincident with the laser beam.[3] The beam enters off axis at a distance x_0 from the rotation center; the vertical distance $y_0 = 0$, ideally. If the disk is now rotated with an angular velocity $\vec{\omega}$, there will be a linear velocity component v_R having the velocity $\vec{v} = \vec{\omega} \times \vec{r}$ of the medium ($\vec{r}$ being the distance from center, $|\vec{r}| \simeq x_0$) along the refracted beam R, which causes drag. The velocity component v_I parallel to the incident beam is also given in Fig. 1.

Parks and Dowell[5] recently generalized the drag formula for arbitrary angles between the velocity

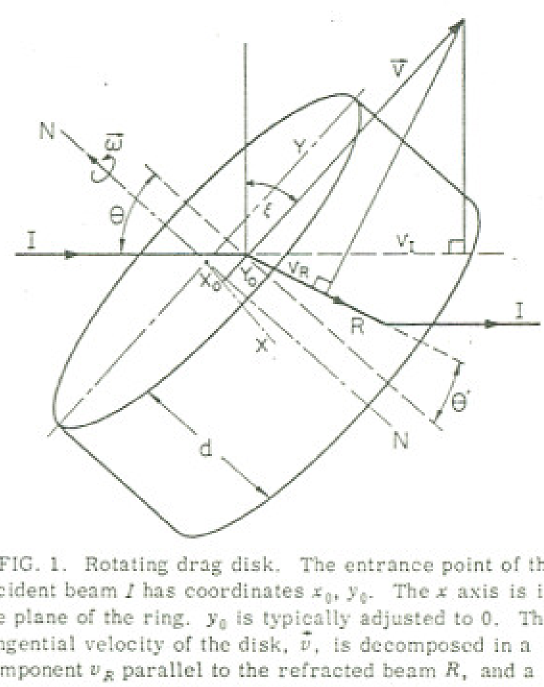

FIG. 1. Rotating drag disk. The entrance point of the incident beam I has coordinates x_0, y_0. The x axis is in the plane of the ring. y_0 is typically adjusted to 0. The tangential velocity of the disk, $\vec{v}$, is decomposed in a component v_R parallel to the refracted beam R, and a component v_I parallel to the direction of the incident beam I.

vector of the medium, and the incident and refracted light beam. With the aid of Fig. 1, and the definition of the drag coefficient α through

$$u = c/n + \alpha v_R, \tag{1}$$

c being the vacuum speed of light and u the phase speed of light in the laboratory system, they derive the expression

$$\alpha = 1 - n^{-2} - \frac{\lambda}{n^2}\frac{dn}{d\lambda}\frac{v_I}{v_R}. \tag{2}$$

For a disk with a linear velocity vector parallel to the surface, application of Snell's law yields (for any tilt θ)

$$v_I = n v_R, \tag{3}$$

and therefore the Lorentz drag results:

$$\alpha_{\rm LO} = 1 - n^{-2} - \frac{\lambda}{n}\frac{dn}{d\lambda}. \tag{4}$$

It should be noted here[1,4,5] that in Zeeman's arrangement, slugs of flint glass or quartz, or columns of water, are moved to and fro in the light beam, such that $v_I = v_R$, in which case the Laub coefficient

$$\alpha_{\rm LA} = 1 - n^{-2} - \frac{\lambda}{n^2}\frac{dn}{d\lambda} \tag{5}$$

holds. The differences appear in the dispersion term, but not in the Fresnel term $1 - n^{-2}$.[6]

To estimate the frequency splitting in a ring laser due to drag, we may simply assume that the drag affects the resonance frequencies via the change of the optical length

$$L = \oint n'(\lambda, v_m)\, dr = \oint [c\,dr/u(n, v_R)]$$

(the contour is taken over the actual path of the closed light beam), such that

$$\Delta f/f = -\Delta L/L \tag{6}$$

[see Eq. (7) in Ref. 3].

The beat frequency due to drag, Δf_D, in a rotating cylinder for arbitrary orientation (directional angles ϕ and ξ) and arbitrary entrance point $P_0(x_0, y_0, z_0 = 0)$ is given as

$$\Delta f_D = \alpha_e \frac{2n^2 d}{\lambda L}\,\omega\,\frac{x_0\cos\xi - y_0\cos\phi}{(1 - \cos^2\phi - \cos^2\xi)^{1/2}} \tag{7}$$

(see Eqs. (11) and (A5) in Ref. 3), where α_e is the experimental value of the drag coefficient α.

Including the Sagnac effect due to the Earth's rotation, Δf_R, we expect a total optical beat frequency

$$\begin{aligned}\Delta f_B &= \Delta f_D(\omega, x_0) + \Delta f_R\\ &= \alpha_e \frac{2n^2 d}{\lambda L}\,\omega\,\frac{x_0\cos\xi - y_0\cos\phi}{(1 - \cos^2\phi - \cos^2\xi)^{1/2}} + b.\end{aligned} \tag{8}$$

Here we indicate that the drag is studied by varying rotation rate $\omega = 2\pi f_m$ and off-axis distance x_0, and that the Sagnac effect is additive and constant, $\Delta f_R = b$.

To determine α_e to a level $< 10^{-3}$, the various quantities entering Eq. (8) have to be assessed to a level of about 10^{-4}.

III. THEORY OF MEASUREMENT AND ERRORS

The combined effect of drag and Sagnac effect has to overcome the lock-in frequency and pulling range, which is generally a few hundred Hertz. To avoid systematic errors due to such undesirable side effects, a series of drag runs are made as Δf_B vs $f_m(x_0 = \text{const})$, and Δf_B vs $x_0(f_m = \text{const})$, and the least-squares-fitted slopes $m_0 = \partial(\Delta f_B)/\partial f_m$ and $m_1 = \partial(\Delta f_B)/\partial x_0$ are used for further analysis. Straight-line fits also allow one to judge whether any residual curvatures due to pulling, etc., exist.

Differentiating Eq. (8) with respect to f_m and x_0 results in

$$\begin{aligned}m_0 &= \alpha_e(4\pi n^2/\lambda L)(d)(x_0\cos\xi - y_0\cos\phi)\\ &\quad\times(1 - \cos^2\phi - \cos^2\xi)^{-1/2}\end{aligned} \tag{8a}$$

and

$$\begin{aligned}m_1 &= \alpha_e(4\pi n^2/\lambda L)(d)(f_m\cos\xi)\\ &\quad\times(1 - \cos^2\phi - \cos^2\xi)^{-1/2},\end{aligned} \tag{8b}$$

i.e., the off-axis distance x_0 enters Eq. (8a) (with its error), whereas the rotation rate f_m enters Eq. (8b) instead (with its error).

Logarithmic differentiation of these equations gives [after rearranging terms, and with the angles of the disk properly set, namely, $\phi = 90°$, and $\tan\xi = \tan\theta_B = n$ (the Brewster angle)]

$$\frac{\Delta\alpha_e}{\alpha_e} = \frac{\Delta m_0}{m_0} - \frac{\Delta x_0}{x_0} + \frac{(n^2+1)\Delta\xi}{n} - \frac{\Delta d}{d} + \frac{\Delta L}{L} + \frac{\Delta\lambda}{\lambda} - \frac{2\Delta n}{n} \tag{9a}$$

and

$$\frac{\Delta\alpha_e}{\alpha_e} = \frac{\Delta m_1}{m_1} - \frac{\Delta f_m}{f_m} + \frac{(n^2+1)\Delta\xi}{n} - \frac{\Delta d}{d} + \frac{\Delta L}{L} + \frac{\Delta\lambda}{\lambda} - \frac{2\Delta n}{n}. \tag{9b}$$

Errors Δy_0 and $\Delta\phi$ enter only as second-order terms.

The error analysis was carried out to the second order, and a variety of checks, including experimental checks, were carried out to ensure that second-order errors are well below 1×10^{-4}.

Of the terms on the right side of Eqs. (9), the first two terms are obtained directly through the statistics of the drag runs; $\Delta\xi$ is a residual adjustment error of the drag disk; the fourth and fifth terms are given through errors in the measurement of disk thickness and the determination of the optical length of the ring; the last two terms are given in the literature.[7,8]

Wavelength. The vacuum wavelength of an I_2-stabilized visible Ne-laser transition is given as $\lambda = 632\,991.39\pm0.02$ pm.[7] We do not stabilize the wavelength in our ring, but since we allow only one axial mode during drag runs, which will be near the peak of the Doppler-broadened Ne line, and since the axial-mode separation is about 90 MHz, we expect an equivalent wavelength uncertainty $|\Delta\lambda/\lambda| = |\Delta f/f| \simeq 2\times10^{-7}$ ($\ll 10^{-4}$). Therefore, in our calculations, we consider $\lambda = 0.632\,991$ μm as exact enough for our purposes.

Index of refraction. Reference 8 gives a dispersion formula for n of fused silica prisms of optical quality from several manufacturers. The differences among the specimens amount to less than 1×10^{-5} in the wavelength range of interest. After correction to vacuum and to $T = +24$ °C (average laboratory temperature during our experiments), we arrive at $n(SiO_2\text{-vacuum, } 24\text{ °C}) = 1.457\,44$, with an error of less than 1×10^{-5}. This number is adopted in our analysis of the theoretical drag coefficient, and assumed to be exact.

Length of ring. A simultaneous excitation of the ring in four axial modes produced the following three difference frequencies as measured with a Hewlett-Packard 524 D counter with plug-ins 525 A ($f<100$ MHz) and 525 C ($f>100$ MHz): $\Delta f_1 = 89\,455.3$ kHz, $\Delta f_2 = 178\,910.0$ kHz ($\simeq 2\Delta f_1$), $\Delta f_3 = 268\,360.6$ kHz ($\simeq 3\Delta f_1$), from which an average fundamental beat frequency $\Delta f = 89\,454.6\pm0.5$ kHz results, with a relative error $\ll 10^{-4}$. We therefore use the value $L = c/\Delta f = 2.997\,92\times10^8/8.945\,46\times10^7 = 3.351\,33$ m, in our analysis. No active stabilization of the perimeter L was introduced. The stability of L is watched on a spectrum analyzer Tektronix (1L20) which is tuned to Δf_1. The very nearly equispaced beat frequencies are an indication that frequency pulling of the axial modes, or similar effects affecting frequencies, are negligible in our set-up.

The above data show that errors in λ, L, and n are negligible at the level of 10^{-4}. To obtain an estimate of the overall error, we treat the remaining uncertainties as random and uncorrelated, with the result

$$\frac{\Delta\alpha_e}{\alpha_e} = \left[\left(\frac{\Delta m_0}{m_0}\right)^2 + \left(\frac{\Delta x_0}{x_0}\right)^2 + \frac{(n^2+1)^2\Delta\xi^2}{n^2} + \left(\frac{\Delta d}{d}\right)^2\right]^{1/2} \tag{10a}$$

or

$$\frac{\Delta\alpha_e}{\alpha_e} = \left[\left(\frac{\Delta m_1}{m_1}\right)^2 + \left(\frac{\Delta f_m}{f_m}\right)^2 + \frac{(n^2+1)^2\Delta\xi^2}{n^2} + \left(\frac{\Delta d}{d}\right)^2\right]^{1/2}. \tag{10b}$$

The symbol Δ indicates the rms deviation of the quantity.

IV. DRAG SITE

The experimental approach follows rather closely the one described in Ref. 3. The same plasma tube and approximately the same ring perimeter are used, as well as similar techniques in adjusting and operating the ring. We will therefore restrict ourselves to detail refinements, where indicated.[9]

Drag site. A complete, more massive and more accurate reconstruction of the holder of the Homosil $\lambda/20$-fused silica drag disk was done. The disk was inserted into an x-y translator (Lansing model No. 20.127) with 10^{-4}-in. (2.54 μm) resolution in x ($=x_0$) and y. The total travel is about 1 in. The tilt is adjustable with a resolution of 10 arcsec. The orientation angle ϕ was adjusted to within 5 arcmin by rotating the whole drag site until the reflected beam was in a vertical plane. This was verified by bringing the reflected beam on a line at the ceiling which was obtained by plumbing onto the corresponding ring-laser arm. As mentioned above, $\Delta\phi$ enters as a second-order error, and its effect on $\Delta\alpha_e$ is negligible.

The adjustment of the Brewster angle required much more care. In this procedure, the rf excitation of the plasma tube was modulated with a 1000-Hz signal; the reflected beam off the drag disk was passed through a laser-line filter [University Laboratories 1 UL-3021 (100 Å = 10-nm bandwidth)] and a polarizer, and the minimum was observed after detection of the light intensity with a photodiode and filtering through an active band filter with a bandwidth of 200 Hz (Hewlett-Packard wave analyzer HP 310). In this way the Brewster angle could be adjusted to within $\Delta\xi = \pm 20$ arcsec. This gives rise to an error $(n^2+1)\Delta\xi(\text{rad})/n = 2.1\times10^{-4}$.

The thickness of the disk, d, was determined as $d = (0.5029\pm0.0001)$ in. $= (1.2774\pm0.0003)$ cm. The error term in d is therefore $\Delta d/d = 2\times10^{-4}$.

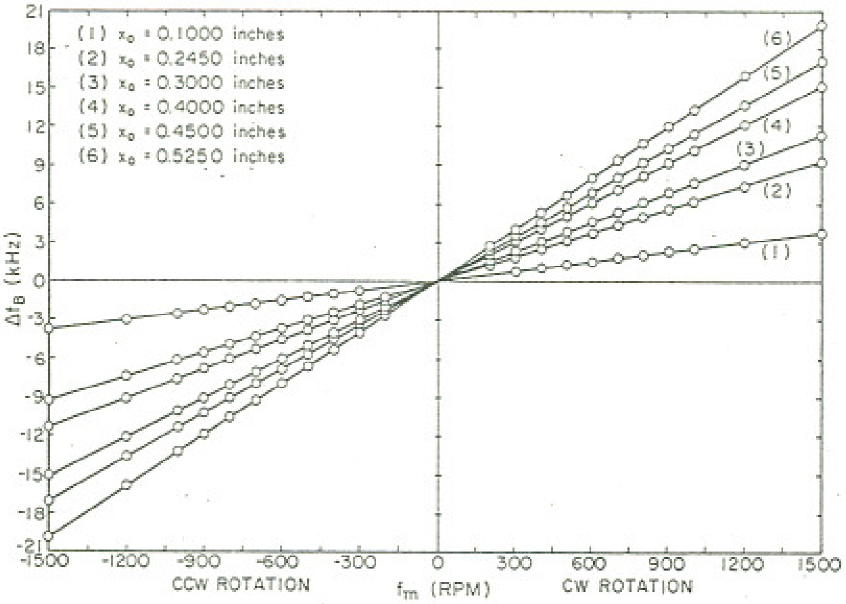

FIG. 2. Beat frequency Δf_B vs rotation rate f_m of the drag disk, with the displacement x_0 ranging from 0.1 to 0.525 in. Counterclockwise (CCW) rotation is assigned a negative rate. An individual point is obtained by counting for typically 3 to 6 min. The statistical errors of the points are smaller than the dot size.

V. DRAG

Beat frequency and rotation rate. The ring laser is adjusted to single-mode operation by inserting an iris in the beam, and lowering the rf input until Δf_1 vanishes. Its output is detected with a silicon photodiode (Fairchild FPM 200). The preamplified signal is passed through a high-pass filter (corner frequency 500 Hz), then through a Tektronix 547 oscilloscope with 1A7A plug-in. There the bandpass filter (RC filters) is set to 100 Hz and 300 kHz, respectively. The scope therefore serves as monitor, post-amplifier, and additional filter. The output spectrum is monitored with a panoramic analyzer (Singer Model MF-5) and fed into a wave analyzer (Hewlett Packard 310 A) with a 1-kHz bandwidth. A counter (General Radio 1151-A) counts the beats during 10-sec intervals. The time base and gating signals from this counter also synchronize the counter for the rotation rate. Thus no error is introduced in measuring the ratio $\Delta f_B/f_m$, or the slope m_0. In addition, the time base has been found to have errors well below 10^{-4}. Beat frequencies are between 0.8 and 53 kHz, and rotation rates between 200 and 3500 rpm.

Off-axis distance x_0. To determine this quantity, the center of rotation of the disk has to be found. The uncertainty was about 4×10^{-4} in. $=10$ μm. Such an error would be sizeable, as the mean off-axis distance is about $x_0 = 1$ cm in the runs, so that $\Delta x_0/x_0 \simeq 10\times10^{-4}$. Fortunately, in the runs of Δf_B vs x_0, the slope $m_1 = \partial(\Delta f_B)/\partial x_0$ [Eq. (8b)] is independent of any error in the location of the center of rotation. What remains is the accuracy of the micrometer itself, for setting x_0 including slack. The latter problem was checked by repeatedly setting the disk to the same nominal distance x_0 and measuring the beat frequency. It appears that slack introduces an error $<1\times10^{-4}$. The manufacturer confirms that the accuracy of the micrometer is better than its resolution. Therefore we did not include this error in our analysis. The range of x_0 in our experiments is 0.1 to 0.525 in.

The runs Δf_B vs f_m and Δf_B vs x_0 are thus complementary, in the sense that the first experiment is sensitive to an error in the location of the center of rotation, whereas the second experiment is sensitive to an error in the determination of the rotation rate.

VI. RESULTS

For each setting of x_0 and f_m, 20 to 40 data recordings were made of Δf_B and f_m, each covering a 10-sec run. The mean values, $\overline{\Delta f_B}$ and $\overline{f_m}$, are entered as a point in Figs. 2–4. Seventeen sets of runs were made altogether, with $\overline{\Delta f_B}$ vs $\overline{f_m}$ for six different off-axis distances x_0 (Fig. 2), and with $\overline{\Delta f_B}$ vs x_0 for 11 different rotation rates f_m. Counterclockwise rotation is plotted as a negative rotation rate.

A typical 10-sec run has a statistical rms error of Δf_B of about ±6 Hz, and of f_m of about ±0.2 rpm. The averages over 20–40 runs therefore have errors of about ±1 Hz and ±0.03 rpm, respectively. The statistics are, furthermore, drastically improved by least-squares fitting of straight lines, as outlined above. The errors in the points cannot be made visible in Figs. 2–4, as they are well below 10^{-3}. The fits also showed that the residuals are randomly distributed around the

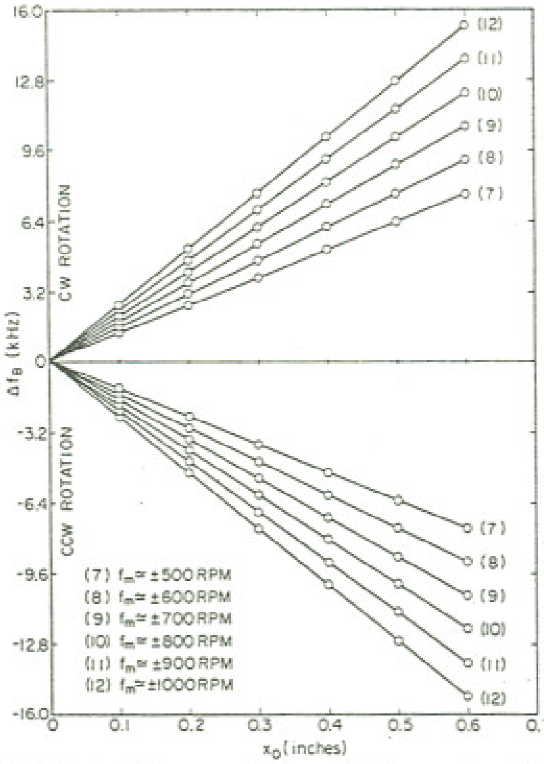

FIG. 3. Beat frequency Δf_B vs displacement x_0 of the beam off the axis of the drag disk, with the rotation rate ranging from 500 to 1000 rpm. Clockwise and counterclockwise rotation is employed for each roation rate.

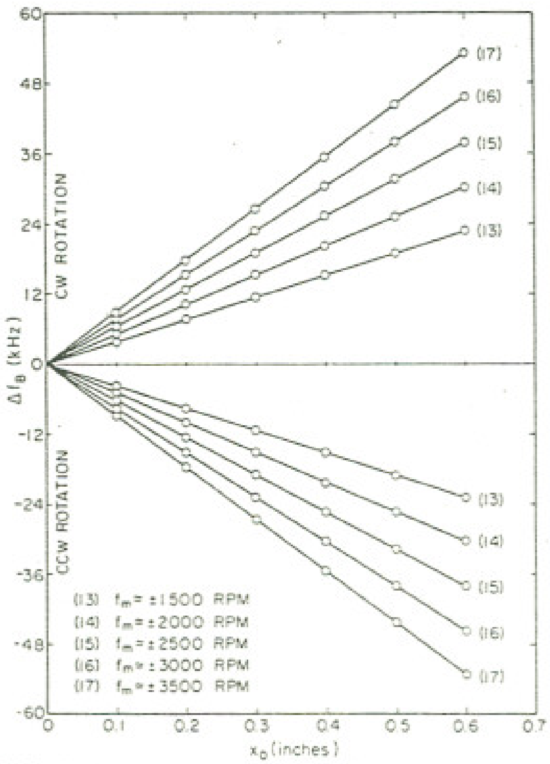

FIG. 4. Same as Fig. 3, except that rotation rates of 1500 to 3500 rpm are used.

TABLE I. Data from 17 drag runs. All 17 measurements: $\overline{M} = 25.316 \pm 0.005$ Hz/rpm in.; 15 best measurements: $\overline{M} = 25.315 \pm 0.003$ Hz/rpm in., $\overline{\alpha}_e = 0.542\,37 \pm 0.000\,07$.

Run no.	Parameter value	Slopes	M (Hz/rpm in.)	α_e
	x_0 (in.)	$m_0 = \partial(\Delta f_B)/\partial f_m$ (Hz/rpm)		
1	0.1000	2.5368	25.368	0.5435
2	0.2450	6.2046	25.325	0.5426
3	0.3000	7.5928	25.309	0.5422
4	0.4000	10.1230	25.308	0.5422
5	0.4500	11.3922	25.316	0.5424
6	0.5250	13.2830	25.301	0.5421
	$\overline{f}_m$ (rpm)	$m_1 = \partial(\Delta f_B)/\partial x_0$ (Hz/in.)		
7	500.7	12 666	25.297	0.5420
8	600.8	15 207	25.311	0.5423
9	701.9	17 773	25.321	0.5425
10	801.7	20 285	25.303	0.5421
11	903.1	22 861	25.314	0.5424
12	1003.0	25 410	25.334	0.5428
13	1500.7	38 022	25.336	0.5428
14	2000.7	50 646	25.314	0.5424
15	2501.0	63 285	25.304	0.5421
16	3002.4	76 054	25.331	0.5427
17	3502.3	88 528	25.277	0.5416

straight lines. The absolute average of all residuals of the measured points (each corresponding to about 2-min measurement time) is 6 Hz. No trend is visible in the data. Only 4 points of the 262 points deviate by more than 20 Hz from the straight lines.

We note here that the intersections of the straight lines with the $x_0 = 0$ or $f_m = 0$ axes are not at zero; indeed, the average of all 17 fits gives 48.2 ± 0.6 Hz, compared to a calculated Sagnac effect of 43.4 Hz. This agreement, within a few Hertz, of an extrapolated intersection (the lowest actually measured beat frequency is 812 Hz) shows that a bias in the slopes is unlikely.

To obtain a general information of the goodness of fit, we evaluated the correlation coefficient r. In 16 of the 17 measurements, $(1-r) < 1 \times 10^{-4}$ (a perfect fit gives $r = 1$). Table I summarizes all data obtained. In runs 1–6, x_0 was adjusted from 0.1 in. up to 0.525 in. (second column); the least-squares fitted slopes $m_0 = \partial(\Delta f_B)/\partial f_m$ are given in column 3. In runs 7–17, f_m was adjusted to 500.7 rpm up to 3502.3 rpm, and correspondingly the slopes $m_1 = \partial(\Delta f_B)/\partial x_0$ are given in column 3. An intercomparison of all slopes is facilitated by calculating $M = m_0/x_0$, or $M = m_1/f_m$ which, according to Eq. (8), should result in the same value for all runs (set $y_0 = 0$, $\phi = 90°$, $\xi = \theta_B$).

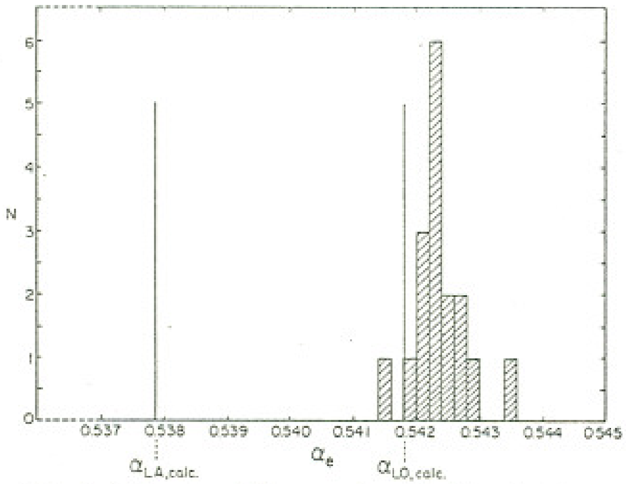

FIG. 5. Histogram of the experimental determinations of the drag coefficient α_e. Conversion of the slopes $M=\partial\Delta f_B/\partial f_m=\partial\Delta f_B/\partial x_0$ to α_e is done with Eq. (11). Systematic errors are not taken into account. The histogram gives an impression of the random error in this experiment. Calculated values of the Lorentz drag and the Laub drag (for fused silica at 633 nm) are included for comparison.

The fourth column displays the 17 estimates of M. It is noteworthy that the two sets of runs are not systematically different (no systematic error in the setting of x_0, or in evaluating f_m, see Sec. V). The extreme deviations of M occur at the largest rotation rate and the smallest off-axis distance x_0. In the analysis, we eliminate those two values. The remaining 15 determinations of M then give the result

$$\overline{M}=(25.315\pm 0.003)\ \mathrm{Hz/rpm\ in.}$$

The individual values of the drag coefficient α_e are calculated from Eq. (8) with $\phi=90°$, $y_0=0$, $\tan\theta_B=n$ as

$$\alpha_e=\frac{\lambda L}{4\pi d n}M(\mathrm{m}^{-1})=0.021\,425\,M\left(\frac{\mathrm{Hz}}{\mathrm{rpm\ in.}}\right), \quad (11)$$

with $\lambda=6.329\,91\times 10^{-7}$ m, $n=1.457\,06$ (in air), $L=3.351\,33$ m (Sec. III), $d=1.2774\times 10^{-2}$ m (Sec. IV), and the values of M from Table I. The results are tabulated in the last column of Table I, and plotted in a histogram in Fig. 5. The best value of α_e is derived from the histogram (omitting the two outlying data), as

$$\overline{\alpha_e}=0.542\,37\pm 0.000\,07,$$

where the given error is the statistical error of the average value in Fig. 5.

VII. COMPARISON TO THEORY

Since our experimental arrangement satisfies Eq. (3), the Lorentz-drag is expected to hold in a linear drag. To evaluate it through Eq. (4), the dispersion of fused quartz at $\lambda=633$ nm and at $T=+24$ °C is obtained from Ref. 8 through differentiation of the dispersion formula, and after corrections for temperature and the dispersion of air are applied. The value $dn/d\lambda=-0.029\,02$ ($\mu\mathrm{m}^{-1}$) was adopted.

The Lorentz drag is then calculated in our experiment via Eq. (4) as

$$\alpha_{LO}=0.541\,82,$$

with negligible uncertainty.

For a significant comparison with $\overline{\alpha_e}$, we recall the error Eq. (10). The overall error due to the statistics of the slopes is $(\Delta M/M)=7\times 10^{-5}/0.54=1.2\times 10^{-4}$ (Sec. VII) which replaces the error terms $\Delta m_0/m_0$ and $\Delta m_1/m_1$. The error in d is assessed as (Sec. IV) $\Delta d/d=2\times 10^{-4}$. The Brewster angle adjustment contributes (Sec. IV) 2.1×10^{-4}. If we further estimate the error terms $\Delta x_0/x_0\simeq 2.5\ \mu\mathrm{m}/1\ \mathrm{cm}\simeq 2.5\times 10^{-4}\simeq \Delta f_m/f_m$, error propagation [Eq. (10)] gives

$$\Delta\overline{\alpha}_e/\overline{\alpha}_e\simeq 4\times 10^{-4},$$

or the experimental value

$$\alpha_e=0.5424\pm 0.0002.$$

VIII. DISCUSSION

The relative difference between the observed drag and the Lorentz drag is $(\alpha_e-\alpha_{LO})/\alpha_e=10\times 10^{-4}$; it amounts to about twice the estimated rms error of the experiment. Thus, a discrepancy cannot seriously be claimed. From this situation, the following conclusions can be drawn:

(i) We verified with high accuracy that the Lorentz-drag equation is applicable to a drag experiment in which the velocity of the dragging medium is tangential to the interface.

(ii) The fact that the drag was accomplished by rotation of the medium rather than by linear translation appears to be immaterial. Indeed, a discussion of the transverse Doppler effect shows that it would not affect the Lorentz drag at this level of accuracy (Ref. 3).

(iii) The fact that the result was obtained with a ring laser as opposed to a linear (classical) arrangement, seems to be of no consequence either. Equation (6) in Sec. II appears to hold.

(iv) Specific comments on the possibility that the drag coefficient in a ring laser may be different from the Fresnel-Fizeau (or Lorentz) drag as made by Post[10] can be answered that, at least to accuracies of a few hundred ppm, drag is indistinguishable from Lorentz drag.

ACKNOWLEDGMENT

We thank H. Hall for his excellent workmanship in construction of the drag site and the mirror holders; also T. J. Boehm and J. L. Tandon for active help and for numerous discussions. One of us (W.K.S.) acknowledges a part-time assistantship provided by the School of Electrical Engineering.

---

*Present address: Centre d'études d'électronique des solides, Université des Sciences et Techniques du Languedoc, 34060 Montpellier Cédex, France.

†Present address: AFAL/RWA-3, Wright Patterson AFB, Ohio 45433.

[1]H. Fizeau, Ann. Chem. Phys. 57, 385 (1859); A. A. Michelson and E. W. Morley, Am. J. Sci. 31, 377 (1886) (Note: This closed light-beam experiment encloses a finite area!); P. Zeeman *et al.* wrote eight papers about the drag, which appeared in the Proceedings of the Royal Academy of Sciences of Amsterdam. English translations of the four most significant papers appeared in Proc. R. Acad. Sci. Amsterdam 17, 445 (1914); 18, 398 (1916) (drag in water); 22, 512 (1920) (drag in quartz); 23, 1402 (1922) (drag in flint glass).

[2]W. M. Macek, J. R. Schneider, and R. M. Salamon, J. Appl. Phys. 35, 2556 (1964).

[3]H. R. Bilger and A. T. Zavodny, Phys. Rev. A 5, 591 (1972); see also A. T. Zavodny, thesis (Oklahoma State University, 1970) (unpublished).

[4]The errors appear to be quite dependent on the quality of the drag material. Zeeman's data with water and flint glass appear to have relative errors of about 0.6% and 2%, respectively.

[5]W. F. Parks and J. T. Dowell, Phys. Rev. A 9, 565 (1974).

[6]In Massey and Siegman's arrangement (Report No. 1812, Hansen Laboratories, Stanford University, 1969) where a beam enters the equatorial plane of a spinning sphere under the Brewster angle, the drag coefficient is given by $\bar{\alpha}=1-n^{-2}-2(n^2+1)^{-1}(\lambda/n)(dn/d\lambda)$ in first order. The velocity of the medium varies along the beam path, as well as v_I, but v_R stays constant.

[7]G. R. Hanes and K. M. Baird, Metrologia 5, 32 (1969).

[8]I. H. Malitson, J. Opt. Soc. Am. 55, 1205 (1965); see also *American Institute of Physics Handbook*, 3rd ed., edited by D. E. Gray (McGraw-Hill, New York, 1972), Sec. 6, pp. 6–28.

[9]For further details, see W. K. Stowell, thesis (Oklahoma State University, 1974) (unpublished).

[10]E. G. Post, Rev. Mod. Phys. 39, 475 (1967).